Excitation of a Single Atom with Exponentially Rising Light Pulses

Syed Abdullah Aljunid,[1] Gleb Maslennikov,[1] Yimin Wang,[1] Hoang Lan Dao,[2]
Valerio Scarani,[3] and Christian Kurtsiefer[3,*]

[1]*Centre for Quantum Technologies, National University of Singapore, 3 Science Drive 2, Singapore 117543*
[2]*Faculty of Science and Technology, University of Twente, P.O. Box 217, 7500 Enschede, The Netherlands*
[3]*Center for Quantum Technologies and Department of Physics, National University of Singapore,*
3 Science Drive 2, Singapore 117543

We investigate the interaction between a single atom and optical pulses in a coherent state with a controlled temporal envelope. In a comparison between a rising exponential and a square envelope, we show that the rising exponential envelope leads to a higher excitation probability for fixed low average photon numbers, in accordance with a time-reversed Weisskopf-Wigner model. We characterize the atomic transition dynamics for a wide range of the average photon numbers and are able to saturate the optical transition of a single atom with ≈ 50 photons in a pulse by a strong focusing technique.

In order to compose more and more complex networks of quantum systems for quantum information processing, efficient interfaces between different physical systems are required [1–3]. An important representative of such an interface are two-level atoms coupling to photons that can propagate between distant atoms.

The fundamental processes for exchanging information between atoms and photons are emission and absorption. While capturing an emitted photon from an atom can usually be done with high efficiency, the reverse process is more challenging, since the field strength of a single photon is very weak. Accomplishing a high excitation probability for an atom from a single photon is thus quite challenging. It is common to solve this problem in the context of cavity QED, where the field strength of single photons at the location of the atom is dramatically increased by using optical cavities with small mode volumes [4]. However, sophisticated dielectric coatings are required to decouple the cavity from environmental losses which compromise the scaling of such systems. To relax the coating requirements, the mode volume has to be further decreased, and several experimental efforts target this issue [5]. Placing an atomic two-level system in a strongly focused mode also increases the electrical field of a photon, and can lead to reasonably strong interaction [6–8] even without an optical cavity. In this case, the emission and absorption of photons are not affected by the presence of artificial boundary conditions, and the absorption depends only on the *overlap* of spatial and frequency modes of the light field with atomic transition modes. Considering only dipole-allowed transitions and a lifetime-limited spectral absorption profile, it has been shown that near perfect excitation probability can be achieved with a wave packet that has an exponentially rising temporal envelope with a characteristic time on the order of the decay time of the excited atomic state [9,10]. Temporal shaping of photons is not only important for

boosting atom-photon interactions in free space, but also in the context of cavity QED based networks [11,12] and quantum memories with atomic ensembles [13].

In this Letter we investigate the effect of temporal shaping of light pulses on the excitation probability of a closed cycling two-level transition in a single ^{87}Rb atom.

The experimental setup is schematically shown in Fig. 1. A single atom is trapped in a far-off resonant optical dipole trap (FORT) at the focus of two confocally positioned aspheric lenses. The FORT is loaded from a magneto-optical trap (MOT) holding $\approx 10^4$ atoms. A collisional
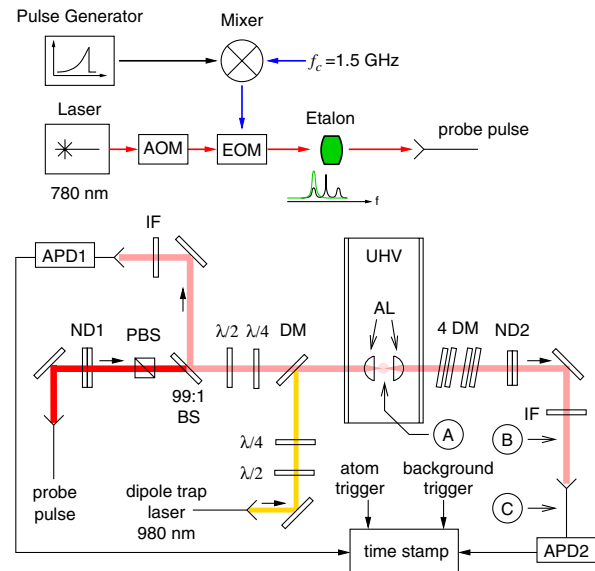

FIG. 1 (color online). Top: Preparation of pulses with controllable waveform. Bottom: Setup for transmission and reflection measurement of light by a single atom. UHV: ultra high vacuum chamber, AL: aspheric lenses with full $\mathrm{NA} = 0.55$ and focal length $f = 4.51$ mm; PBS, polarizing beam splitter; ND1,2, stacks of neutral density filters; $\lambda/2$, $\lambda/4$, wave plates; DM, dichroic mirrors; IF, interference bandpass filters centered at 780 nm.

blockade mechanism ensures that either zero or one atom is trapped at any instance [14]. A probe beam is delivered from a single mode optical fiber and defines the focused light mode that is coupled to the atom. This gives the probe beam a Gaussian spatial mode with a characteristic waist $w_L = 1$ mm at the focusing lens ($f = 4.51$ mm).

If no atom is present in the trap, the second lens recollimates back the probe beam. It then passes through several filters and finally is coupled to another single mode fiber with 72% efficiency (from B to C in Fig. 1). The other end of the fiber is attached to a silicon avalanche photodiode (APD2) operating in a passively quenched photon counting mode (dead time about 3 μs, quantum efficiency 55%). Backscattered light (and atomic fluorescence from the MOT beams) is also collected into another single mode fiber that is coupled to a second avalanche photodiode (APD1). Both photodiode signals and a reference signal for the optical excitation pulses are time stamped with a resolution below 1 ns for further analysis.

Optical excitation pulses are prepared from a continuous laser with a combination of an acousto-optical modulator (AOM) and an electro-optical modulator (EOM). The pulse envelope (rising exponential or approximately square) is determined by modulating the radio frequency amplitude of the EOM. The first red optical sideband of the light leaving the EOM is extracted with a series of three temperature-tuned etalons (line width $\approx$ 460 MHz), suppressing the optical carrier by about 60 dB. Details can be found in Ref. [15].

The average number of photons $\langle N \rangle$ in each pulse was varied by inserting calibrated neutral density filters (ND1), and determined from a histogram of detection times of the forward photodiode (see Fig. 2 for two typical pulses). For that we use the expression $\langle N \rangle = r_d/(\eta_l \eta_{ND2})$, where r_d is the fraction of all pulses that cause photodetection events in APD2, η_{ND2} is the transmission of neutral density filter ND2, and $\eta_l = 0.30 \pm 0.02$ the system efficiency capturing reflection and coupling losses from A to C (see Fig. 1)
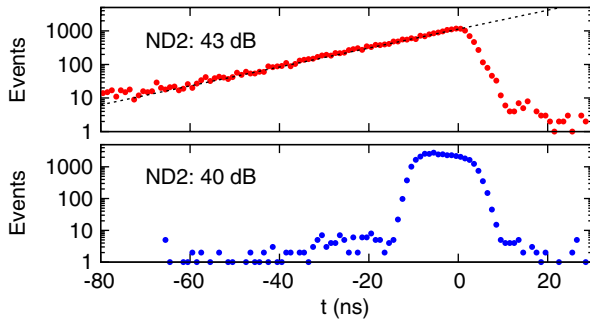

FIG. 2 (color online). Histograms of detection times with respect to a pulse edge for 1.5×10^7 excitation pulses in time bins of 1 ns. Top: exponentially rising pulse with $\tau = 15$ ns and mean photon number $\langle N \rangle = 110 \pm 6$, with an exponential fit (dashed line). Bottom: Reference pulse with $\tau = 15$ ns and $\langle N \rangle = 104 \pm 5$.

and the quantum efficiency of APD2. To avoid dead time effects of the photodetector, η_{ND2} was chosen between -25 and -51 dB such that $r_d \lesssim 1\%$.

We start the excitation experiment once an atom is loaded from the MOT into the FORT, identified by its fluorescence detected with APD1, with 5 ms of molasses cooling. Then we optically pump the atom to $5S_{1/2}|F = 2, m_F = -2\rangle$ with a circularly polarized optical pumping light for 10 ms. This is followed by a train of 100 optical probe pulses separated by 12 μs to minimize dead time effects of the photodetectors. To keep the central optical frequency of the pulse resonant with the $5S_{1/2}|F = 2, m_F = -2\rangle \rightarrow 5P_{3/2}|F = 3, m_F = -3\rangle$ transition, Zeeman and ac Stark shift in the trap were calibrated in an independent probe transmission measurement with cw light.

After probing, we verify the presence of the atom by fluorescence from the molasses beams for 20–30 ms, which also removes the recoil energy the atom acquired during the probe period. If the atom was not lost, the probing sequence is repeated. Otherwise, the same sequence of probe pulses is recorded for 3 s as reference to measure the average photon number $\langle N \rangle$ in the pulse.

The probability $P_e(t)$ of an atom being in the excited state at any time t can be directly assessed by the fluorescence detected in backwards direction with APD1, because there is no interference between backscattered and excitation light. We sort the photodetection events into time bins of width $\Delta t = 1$ ns with respect to the pulse edge. The total number of excitation pulses N_T that are sent to an atom while it is in the trap is independently measured by a time stamp unit as shown in Fig. 1. The excitation probability in time bin t is then given by

$$P_e(t) = N_d(t)/(\Gamma_p \Delta t \eta_r N_T), \tag{1}$$

where $N_d(t)$ is the number of detected fluorescence events in the same time bin, and $\eta_r = 0.30 \pm 0.02$ is a product of the quantum efficiency of detector APD1 and the transmission through all optical components from the atom to the detector. The atomic decay rate into the excitation pulse mode Γ_p is proportional to the free space spontaneous decay rate Γ of the excited state,

$$\Gamma_p = \eta_p \Gamma, \tag{2}$$

η_p being the spatial overlap parameter between the atomic dipole and excitation pulses.

Following the analysis of our experimental configuration in [16], the spatial overlap can be expressed in terms of the scattering ratio R_{sc}, which depends on the focusing strength $u := w_L/f$ as

$$\eta_p = \frac{R_{sc}}{4} = \frac{3}{16u^3} e^{2/u^2} \left[\Gamma\left(-\frac{1}{4}, \frac{1}{u^2}\right) + u\Gamma\left(\frac{1}{4}, \frac{1}{u^2}\right) \right]^2, \tag{3}$$

where w_L is the input beam waist, f the focal distance of the coupling lens, and $\Gamma(a, b)$ the incomplete gamma function. The parameter $u = 0.22$ in our experiment would
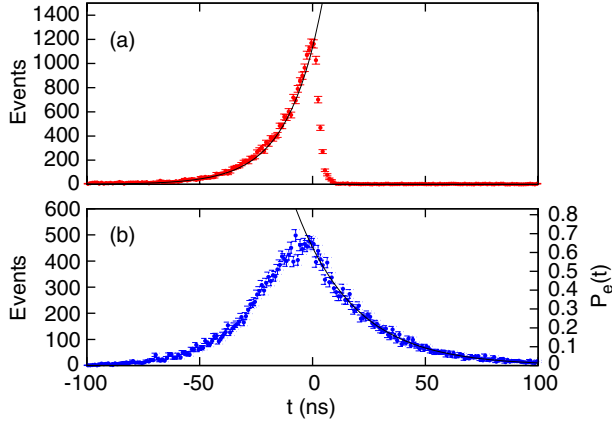
FIG. 3 (color online). Exponentially rising excitation pulse (a) and atomic fluorescence detected in backward direction (b). The left-hand axis depicts the histogrammed photoevents in a 1 ns wide time bin, the right-hand axis on the fluorescence plot the excitation probability derived from it (see text for details). Error bars indicate Poissonian counting statistics. The solid lines indicate exponential fits with time constants of $\tau = 15.4$ ns for the excitation pulse and $\tau = 26.2$ ns for the decay in the fluorescence.

FIG. 4 (color online). Time-dependent atomic excitation probability P_e for pulses with a large average photon number $\langle N \rangle$, leading to Rabi oscillations. Solid lines represent simulations according to the model in [10].

correspond to $\eta_p = 0.03$. To verify this number, we recorded the photodetection rate in backward detector APD1 from a free decay of a single atom excited with a high probability by a short excitation pulse. This provides a lower bound $\eta_p = 0.027$ for the spatial overlap parameter, which is very close to the calculated value.

Figure 3(b) shows the histogram of detection events for an exponentially rising envelope with a characteristic time $\tau = 15$ ns for $N_T = 2\,103\,400$ pulses, together with the derived instantaneous excitation probability $P_e(t)$. As a reference, Fig. 3(a) shows the histogram of forward detection events after the atom was lost (with $\eta_{ND2} = -43$ dB) for $N_T \approx 1.5 \times 10^7$ pulses from which we determined the average photon number $\langle N \rangle = 104.1 \pm 4.3$ in the excitation pulse as described previously.

During the increasing pulse amplitude, the photoevents in backward direction also increases exponentially. The atomic population seems to follow the excitation pulse, indicating that we are still in the regime of coherent scattering for $\langle N \rangle \approx 100$. With this power, we can transfer $\approx 70\%$ of the atomic population to the excited state. After the excitation field is switched off, the atomic excited state population starts to decay, leading to an exponentially falling amplitude of light field in accordance with the Weisskopf-Wigner model [17]. We observe atomic fluorescence during the rising excitation pulse—however, in an exact time reversal of the Weisskopf-Wigner model, one would expect no outgoing field component during that time [18,19]. Because of the limited overlap of the spatial modes for excitation and emission in our experiment, the destructive interference between these modes necessary for suppression of the scattering is incomplete, providing an
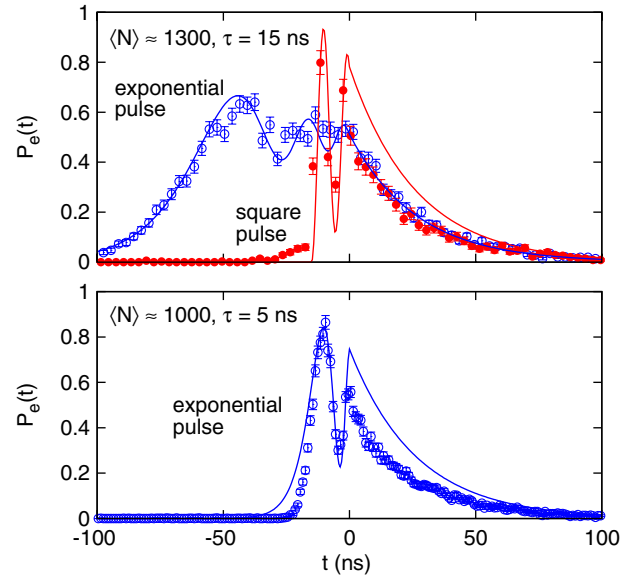
explanation of why we still are able to observe fluorescence at that time.

With increasing $\langle N \rangle$ in the excitation pulse, the response of the atom becomes nonlinear, and eventually the atomic population will undergo Rabi oscillations. Figure 4 shows such oscillations in atomic fluorescence for both square and exponential pulses with $\tau = 15$ ns for $\langle N \rangle \approx 1300$ (top), and for an exponential pulse with $\tau = 5$ ns (bottom). For $\tau = 15$ ns, the oscillation is more pronounced for a square pulse, since, during the long rise time of the exponential pulse, the probability of losing coherence due to spontaneous emission is larger. The deviation from the theoretical model during the free decay of the atom can be explained by finite switch-off times ($\tau_{r/f} \approx 2$ ns) in square pulses (see Fig. 2).

A detailed theoretical analysis of the excitation probability $P_e(t)$ of a two-level atom by a traveling light pulse in free space can be found in [9,10,20]. The atomic excitation varies for different temporal shapes of excitation pulses because $P_e(t)$ is determined by the dynamical coupling strength

$$g(t) = \sqrt{\Gamma_p \langle N \rangle} \, \xi(t). \tag{4}$$

The normalized temporal envelope functions $\xi(t)$ used to model our experiments are

$$\xi(t) = \begin{cases} \frac{1}{\sqrt{\tau}} \exp\!\left(\frac{1}{2\tau} t\right) & \text{for } t < 0 \\ 0 & \text{for } t > 0, \end{cases} \tag{5}$$
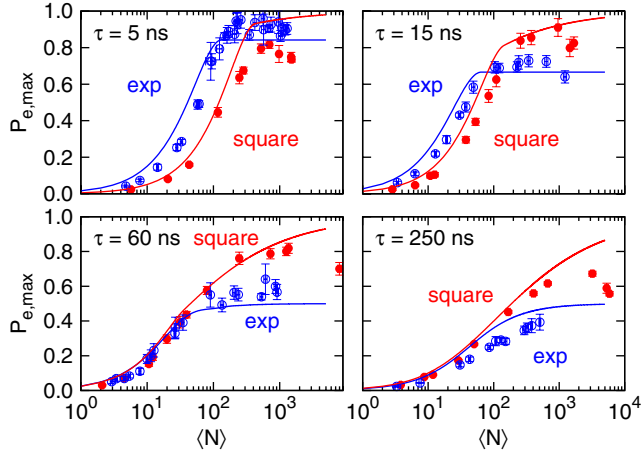
for the rising exponential, and

FIG. 5 (color online).   Maximal atomic excitation probability during a single pulse for different average photon numbers $\langle N \rangle$ and characteristic pulse times τ. Filled circles represent experimental data for exponential, open circles for square excitation pulses. Solid lines represent simulations using a time-dependent coupling strength of Eq. (4) [10], according to which the advantage of the exponential pulse compared to the square pulses decreases with $\langle N \rangle$.

$$\xi(t) = \begin{cases} \frac{1}{\sqrt{\tau}} & \text{for } -\tau \le t \le 0 \\ 0 & \text{otherwise,} \end{cases} \quad (6)$$

for square pulse shape. In this model, the other parameter besides $\langle N \rangle$ determining the coupling strength for a given pulse shape is the pulse duration τ.

To capture the transition between single excitation and Rabi oscillation over a wide range of parameters, we consider the maximal excitation probability $P_{e,\max}$ during the whole pulse period. A few characteristic traces for both pulse shapes are shown in Fig. 5. For long pulses ($\Gamma\tau \gg 1$) and with large $\langle N \rangle$, the atomic population reaches the steady state value of 50% expected for a saturated cw excitation. For shorter pulses, the spontaneous emission probability during the pulse is reduced, and we observe a higher $P_{e,\max}$ for a smaller $\langle N \rangle$; i.e., shorter pulses are better suited to completely excite the atom. In the regime with low $\langle N \rangle$, the exponential pulse shape always leads to a higher excitation probability than the square pulse.

A direct comparison between a square pulse of width τ_s and an exponential pulse of rise time constant $\tau_e = \tau_s$ may not be adequate. We thus compare excitation probabilities with similar photon numbers, $\langle N_e \rangle = 2.75 \pm 0.06$ for the exponential, and $\langle N_s \rangle = 2.10 \pm 0.08$ for the square pulse for τ that maximize $P_{e,\max}$ for $\eta_p = 0.027$. Following [10], maximal excitation would happen for $\tau_e = 24$ ns and $\tau_s = 64$ ns, respectively. The closest available data sets in our measurements of $P_e(t)$ with $\tau_e = 25$ ns and $\tau_s = 60$ ns are shown in Fig. 6. The exponential pulse still leads to larger $P_{e,\max}$ than the square pulse for almost the same average
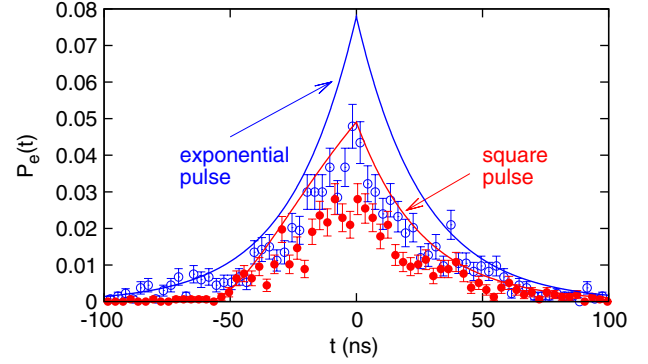

FIG. 6 (color online).   Excitation dynamics for an exponential pulse (filled circles) with $\tau_e = 25$ ns and a square pulse (open circles) with $\tau_{sq} = 60$ ns optimized for the same experimental parameter $\eta = 0.027$, and comparable $\langle N_e \rangle = 2.75 \pm 0.06$ and $\langle N_s \rangle = 2.10 \pm 0.08$, respectively. Solid lines show theoretical predictions for those cases.

photon number. In these measurements, however, there is a significant difference in overall amplitude between the model (solid lines) and the measurements, which we attribute to residual motion of the atom due to thermal motion [21], which leads to the atom experiencing an average field lower than the maximum in the focus, leading to a lower excitation probability. Finite rise or fall time of the excitation pulse should not contribute to these deviations since $\tau_{r/f} \ll \tau_e, \tau_s$.

In summary, we have investigated the interaction of temporally shaped pulses with a single trapped atom and demonstrated that a single atom can be excited with high probability using coherent light pulses with relatively low mean photon number. The excitation of the atom is sensitive to the envelope of the excitation pulse, and we experimentally demonstrated that a rising exponential envelope leads to higher excitation probability in a weak excitation regime, which is compatible with the expectation from a time-reversed Weisskopf-Wigner process. The experiment presented here is in reasonable agreement with a relatively simple model of the excitation process [10], which should provide a good estimation of excitation probabilities of atoms by a single photon in a strongly focused mode in other cases [22,23].

According to the theoretical model for the excitation process [10], the advantage of the exponential pulses should become even more prominent for a larger overlap between excitation and dipole emission modes, as it may be realized in experiments in [18,24], or for a replacement of the coherent states with Fock states of the light field, which will be the ultimate target in an atom-light interaction for quantum information processing purposes.

*christian.kurtsiefer@gmail.com

[1] J. I. Cirac, P. Zoller, H. J. Kimble, and H. Mabuchi, Phys. Rev. Lett. **78**, 3221 (1997).

[2] H. J. Kimble, Nature (London) **453**, 1023 (2008).

[3] L. M. Duan, M. D. Lukin, I. J. Cirac, and P. Zoller, Nature (London) **414**, 413 (2001).

[4] H. J. Kimble, Phys. Scr. **T76**, 127 (1998).

[5] D. Hunger, T. Steinmetz, Y. Colombe, C. Deutsch, T. W. Hänsch, and J. Reichel, New J. Phys. **12**, 065038 (2010).

[6] M. K. Tey, Z. Chen, S. A. Aljunid, B. Chng, F. Huber, G. Maslennikov, and C. Kurtsiefer, Nat. Phys. **4**, 924 (2008).

[7] N. Vamivakas, M. Atature, J. Dreiser, S. T. Yilmaz, A. Badolato, A. K. Swan, B. B. Goldberg, A. Imamoglu, and M. S. Unlu, Nano Lett. **7**, 2892 (2007).

[8] G. Wrigge, I. Gerhardt, J. Hwang, G. Zumofen, and V. Sandoghdar, Nat. Phys. **4**, 60 (2008).

[9] M. Stobińska, G. Alber, and G. Leuchs, Europhys. Lett. **86**, 14 007 (2009).

[10] Y. Wang, J. Minar, L. Sheridan, and V. Scarani, Phys. Rev. A **83**, 063842 (2011).

[11] S. Ritter, C. Nolleke, C. Hahn, A. Reiserer, A. Neuzner, M. Uphoff, M. Mcke, E. Figueroa, J. Bochmann, and G. Rempe, Nature (London) **484**, 195 (2012).

[12] H. P. Specht, J. Bochmann, M. Mcke, B. Weber, E. Figueroa, D. L. Moehring, and G. Rempe, Nat. Photonics **3**, 469 (2009).

[13] M. D. Eisaman, A. Andre, F. Massou, M. Fleischhauer, A. S. Zibrov, and M. D. Lukin, Nature (London) **438**, 837 (2005).

[14] N. Schlosser, G. Reymond, I. E. Protsenko, and P. Grangier, Nature (London) **411**, 1024 (2001).

[15] H. L. Dao, S. A. Aljunid, G. Maslennikov, and C. Kurtsiefer, Rev. Sci. Instrum. **83**, 083104 (2012).

[16] M. K. Tey, G. Maslennikov, T. C. H. Liew, S. A. Aljunid, F. Huber, B. Chng, Z. Chen, V. Scarani, and C. Kurtsiefer, New J. Phys. **11**, 043011 (2009).

[17] V. Weisskopf and E. Wigner, Z. Phys. **63**, 54 (1930).

[18] M. Sondermann, R. Maiwald, H. Konermann, N. Lindlein, U. Peschel, and G. Leuchs, Appl. Phys. B **89**, 489 (2007).

[19] S. Heugel, A. S. Villar, M. Sondermann, U. Peschel, and G. Leuchs, Laser Phys. **20**, 100 (2010).

[20] C. Cohen-Tannoudji, J. Dupont-Roc, and G. Grynberg, *Atom-Photon Interactions: Basic Processes and Application* (Wiley Interscience, New York, 1992), pp. 93–97.

[21] C. Teo and V. Scarani, Opt. Commun. **284**, 4485 (2011).

[22] M. Schug, J. Huwer, C. Kurz, P. Muller, and J. Eschner, Phys. Rev. Lett. **110**, 213603 (2013).

[23] Y. L. A. Rezus, S. G. Walt, R. Lettow, A. Renn, G. Zumofen, S. Gotzinger, and V. Sandoghdar, Phys. Rev. Lett. **108**, 093601 (2012).

[24] A. Golla, B. Chalopin, M. Bader, I. Harder, K. Mantel, R. Maiwald, N. Lindlein, M. Sondermann, and G. Leuchs, Eur. Phys. J. D **66**, 190 (2012).